Bioorganic & Medicinal Chemistry Letters 18 (2008) 5023–5026

Contents lists available at ScienceDirect

Bioorganic & Medicinal Chemistry Letters

journal homepage: www.elsevier.com/locate/bmcl

Structure-guided design of substituted aza-benzimidazoles as potent hypoxia inducible factor-1α prolyl hydroxylase-2 inhibitors

Mike Frohn [a,*], Vellarkad Viswanadhan [a], Alexander J. Pickrell [a], Jennifer E. Golden [a], Kristine M. Muller [a], Roland W. Bürli [a], Gloria Biddlecome [b], Sean C. Yoder [b], Norma Rogers [b], Jennifer H. Dao [a], Randall Hungate [a], Jennifer R. Allen [a]

[a] Department of Chemistry Research and Discovery, Amgen, Inc., One Amgen Center Drive, Thousand Oaks, CA 91320, USA
[b] Department of Hematology, Amgen, Inc., One Amgen Center Drive, Thousand Oaks, CA 91320, USA

ARTICLE INFO

Article history:
Received 12 June 2008
Revised 1 August 2008
Accepted 5 August 2008
Available online 9 August 2008

Keywords:
PHD-2
HIF-1a
Prolyl hydroxylase
Hypoxia
Normoxia
Aza-benzimidazole

ABSTRACT

We report the structure-based design and synthesis of a novel series of aza-benzimidazoles as PHD2 inhibitors. These efforts resulted in compound **22**, which displayed highly potent inhibition of PHD2 function in vitro.

Higher eukaryotes have developed sophisticated mechanisms to enhance uptake and distribution of oxygen in response to hypoxia (below normal cellular pO_2). A central component of this process is oxygen-regulated gene activation mediated by hypoxia inducible transcription factor (HIF).[1] HIF is a heterodimer composed of HIF-α and HIF-β subunits. Three separate genes encoding for the HIF-α subunit (HIF-1α, -2α, and -3α) have been discovered in mammalian cells but only HIF-1α and -2α contain the DNA binding domains essential for transcriptional activity. While HIF-α and HIF-β are constitutively expressed genes, only HIF-α protein levels are regulated by changes in cellular oxygen tension. Under hypoxic conditions, HIF-1α protein is relatively stable, enabling dimerization with HIF-β and subsequent transcription of genes that contain the hypoxia-responsive element (HRE). These genes encode proteins important for erythropoiesis and angiogenesis, as well as various glycolytic enzymes. Together, the regulated expression of these proteins represents a systemic response to reduced oxygen availability.

Interestingly, during normoxia HIF-α protein is continually synthesized and then degraded — a seemingly wasteful process, but one which allows this important regulator to be readily available to respond to changing oxygen levels. HIF prolyl hydroxylases (PHD-1, -2, and -3) are part of a superfamily of non-heme, Fe(II), and 2-oxoglutarate dependent dioxygenases. The PHD enzymes are exquisite oxygen sensors that are responsible for HIF-α stability via O_2-dependent proline hydroxylation. HIF-1α, for instance, becomes hydroxylated on prolines 402 and 564 under normoxia, creating recognition sites for the Von Hippel-Lindau protein complex, which then targets HIF-α for poly-ubiquitination and subsequent proteosomal degradation. As hypoxia ensues, PHD enzymes lack adequate O_2 for catalysis, and HIF-α proline hydroxylation is impaired.

Since HIF stabilization under hypoxia results in expression of genes with possible therapeutic utility, HIF-1α stabilization during normoxia offers an attractive strategy for the treatment of anemia and ischemic diseases.[2] We recently became interested in achieving this goal through the small-molecule inhibition of PHD2, the most broadly expressed isoform and the one most clearly associated with a role in erythropoiesis.[3] The present discussion describes one effort toward rational design of PHD2 inhibitors using a structure-guided approach.

The X-ray crystal structure of isoquinoline **1** bound to PHD2 has recently been reported, which provided the starting point for structure-based design efforts.[4] A schematic representation of critical polar interactions between inhibitor and PHD2 active site residues is shown in Figure 1. The salt bridge between the carboxylate moi-

* Corresponding author. Tel.: +1 805 447 2761, +1 805 551 4632; fax: +1 805 480 1337, +1 805 498 0882.
E-mail address: mfrohn@amgen.com (M. Frohn).

0960-894X/$ - see front matter © 2008 Elsevier Ltd. All rights reserved.
doi:10.1016/j.bmcl.2008.08.012

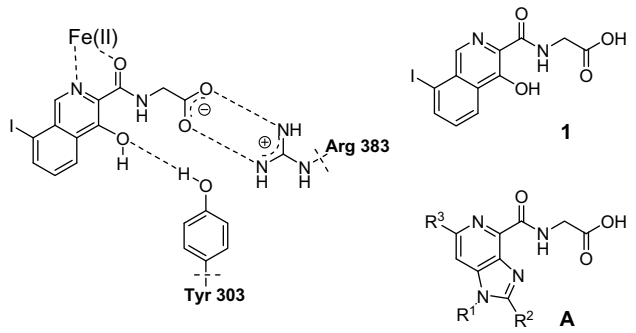

Figure 1. Polar interactions between **1** and PHD2. General structure of designed aza-benzimidazole scaffold.

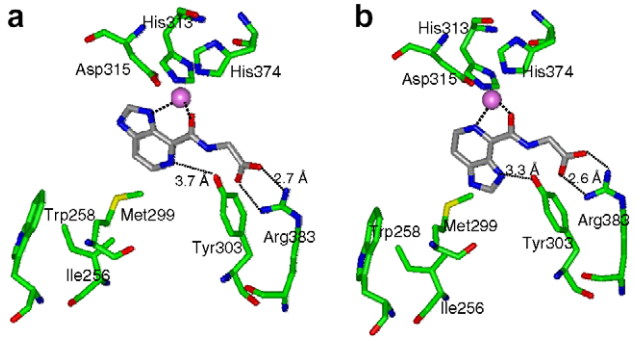

Figure 2. Optimized binding modes of **14** in the active site of PHD2. Fe(II) is shown in pink.

ety of 1 and the guanidino side chain of Arg383, as well as Fe(II) coordination through the isoquinoline nitrogen and amide carbonyl functionalities, appears to be crucial for binding. In addition, Tyr303 serves as an H-bond donor to the isoquinoline hydroxyl.[5]

The aza-benzimidazole scaffold was designed with the goal of discovering structurally diverse PHD2 inhibitors (general structure A, Fig. 1). This structure retains the carboxyl group and Fe(II) binding element of **1**, but replaces the hydroxyl with an imidazole nitrogen. Alkyl substitution(s) at the indicated positions would provide access to hydrophobic areas within the active site. To support the design computationally, a minimally substituted aza-benzimidazole ($R^1 = R^2 = R^3 = H$, **14**) was optimized by molecular mechanics. Overlay of the optimized ground state conformation of this structure with the binding conformation of **1** (as observed in the co-crystal structure), followed by docking of the structure into the active site of PHD2 crystal structure and energetic evaluation showed the potential of this new chemotype.

Importantly, a more detailed molecular modeling analysis of this compound revealed the possibility of two distinct binding modes, each possessing a different orientation of the bicyclic system relative to the amide carbonyl (Fig. 2). The accessibility of the two binding modes appears to be motivated by Fe(II) coordination, with each mode employing a different ring nitrogen for this function. The structure in Figure 2(a) relies on an imidazole nitrogen, while that in Figure 2(b) coordinates through the pyridine nitrogen similar to isoquinoline **1**. Quantum mechanical calculations with the template *N*-methyl-1H-imidazo[4,5-*c*]pyridine-4-carboxamide showed that the minima corresponding to the two modes are energetically very close, with a mild preference (~0.6 kcal) in the gas phase for the conformation shown in Figure 2(a). This energy difference is consistent with molecular mechanics calculations. With this information in hand, a structure–activity relationship (SAR) study was initiated.

Compounds for this study were prepared according to Schemes 1–5. The aza-benzimidazole core was typically constructed by a three-step sequence beginning with 4-chloro-3-nitropyridine 2. S_NAr displacement of the chloride with the requisite amine,[6] reduction of the nitro group, and cyclization by heating in the presence of a carboxylic acid resulted in the bicyclic core structure (general structure **I**, Scheme 1). Synthesis of the C-4 side chain began with the regioselective installation of a nitrile group (general structure **III**), which proceeded by formation of the pyridine N-oxide followed by a modified Reissert–Henze reaction.[7] None of the regioisomeric nitrile was isolated from these reactions.[8]

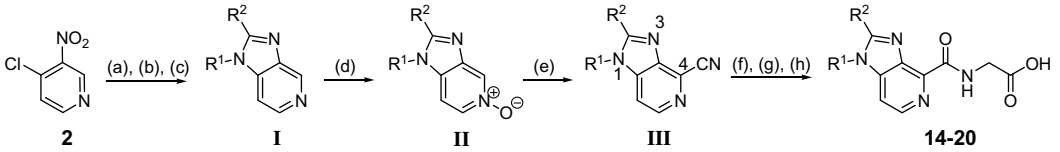

Scheme 1. Synthesis of compounds **14**–**20**. Reagents and conditions: (a) R^1NH_2, concd HCl, H_2O, 2-methoxyethanol, reflux or R^1NH_2, EtOH, rt, 72–99%. (b) Pd-C, H_2, MeOH, 95–99%. (c) R^2CO_2H, 80–120 °C, 78–96%. (d) *m*-CPBA, CH_2Cl_2, rt, 56–89%. (e) *N*,*N*-dimethylcarbamoyl chloride, TMSCN, CH_2Cl_2, rt, 63–91%. (f) concd HCl or 60% H_2SO_4:dioxane (1:1, v/v), 80–95 °C, 23–95%. (g) $H_2NCH_2CO_2Et{\cdot}HCl$, $H_2NCH_2CO_2Bn{\cdot}HCl$, or $H_2NCH_2CO_2{}^tBu{\cdot}HCl$, HBTU, NEt_3 or $(^iPr)_2NEt$, DMF, rt, 47–89%. (h) NaOH (aq), THF or Pd-C, H_2, MeOH or TFA, 9–63%.

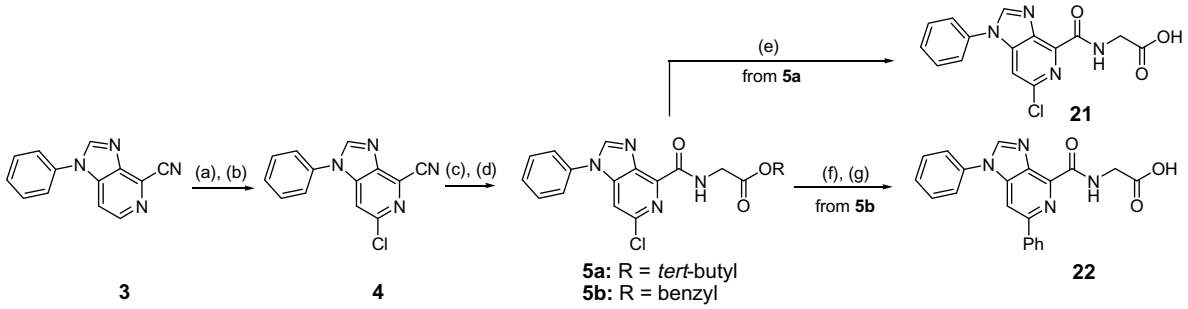

Scheme 2. Synthesis of **21**, **22**. Reagents and conditions: (a) *m*-CPBA, CH_2Cl_2, rt, 50%. (b) $POCl_3$, 100 °C, 95%. (c) 60% aq H_2SO_4: dioxane (1:1, v/v), 90 °C, 40%. (d) $H_2NCH_2CO_2{}^tBu{\cdot}HCl$, 49% or $H_2NCH_2CO_2Bn{\cdot}HCl$, HBTU, $(^iPr)_2NEt$, DMF, rt, 74% (e) TFA, rt, 66%. (f) phenylboronic acid, $Pd(^tBu_2PhP)_2Cl_2$, KOAc, EtOH, 90 °C. (g) NaOH (aq), THF, rt, 6% for 2 steps.

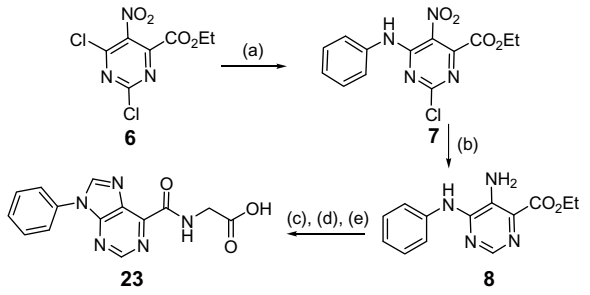

Scheme 3. Synthesis of **23**. Reagents and conditions: (a) aniline, CH_2Cl_2, rt, 48%. (b) Pd (black), H_2 (1 atm), EtOH, rt, 61%. (c) $HC(OEt)_3$, *p*-TSA, 70 °C, 79%. (d) $H_2NCH_2CO_2{}^tBu{\cdot}HCl$, $(^iPr)_2NEt$, dioxane, 90 °C, 82%. (e) TFA, rt, 51%.

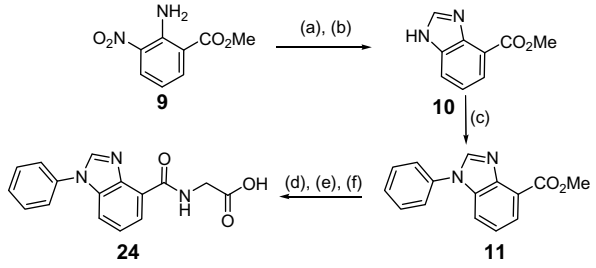

Scheme 4. Synthesis of **24**. Reagents and conditions: (a) Pd-C, H_2, MeOH, 97%. (b) $HC(OEt)_3$, *p*-TSA, reflux, 89%. (c) Phenylboronic acid, $Cu(OAc)_2$, NEt_3, CH_2Cl_2, rt, 13%. (d) KOH (aq), 60 °C, 64%. (e) $H_2NCH_2CO_2Et{\cdot}HCl$, HBTU, $(^iPr)_2NEt$, DMF, rt, 44%. (f) NaOH (aq), THF, rt, 32%.

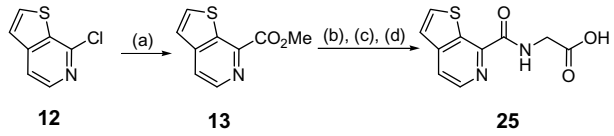

Scheme 5. Synthesis of **25**. Reagents and conditions: (a) $PdCl_2dppp$, CO (25 psi), NEt_3, DMF/MeOH (2:1, v/v), 100 °C, 31%. (b) NaOH (aq), dioxane, rt, 50%. (c) $H_2NCH_2CO_2{}^tBu{\cdot}HCl$, HBTU, $(^iPr)_2NEt$, DMF, rt, 46%. (d) TFA, rt, 65%.

Nitrile hydrolysis under acidic conditions, amide coupling with a protected amino acid, and liberation of the carboxylic acid (reaction conditions dependent upon identity of the ester) completed the synthesis of compounds **14**–**20**.[9]

Analogs carrying substituents at R^3 (**21** and **22**) were constructed in a similar fashion (Scheme 2). Beginning with nitrile **3** (prepared using Scheme 1), a chloride was introduced regioselectively by pyridine N-oxidation and subsequent treatment with $POCl_3$ to give **4**. Selective hydrolysis of the nitrile was accomplished by treatment with H_2SO_4 (aq) in dioxane at 90 °C; the chloride proved stable to these conditions. Amide coupling with a protected amino acid provided an intermediate ester (**5a** or **5b**) that was either converted directly to the corresponding acid (R = *tert*-butyl) to give **21**, or was arylated via Suzuki cross coupling followed by ester saponification (R = Bn) to give **22**. Purine **23** was constructed from ethyl 2,6-dichloro-5-nitropyrimidine-4-carboxylate (**6**). Chemoselective displacement of the C-6 chloride with aniline followed by tandem nitro reduction/chloride removal using heterogeneous hydrogenation conditions (palladium black) resulted in pyrimidine **8**. Formation of the imidazole ring with subsequent side chain elaboration as detailed above finished the synthesis (Scheme 3).

Benzimidazole **24** was prepared by a slightly different strategy. First, the N–H benzimidazole **10** was assembled from methyl 2-amino-3-nitrobenzoate (**9**) using standard chemistry. N-arylation under the influence of $Cu(OAc)_2$ with phenylboronic acid gave a mixture of regioisomeric products, of which **11** was isolated as the major component.[10] Elongation of the C-4 side chain provided **24** (Scheme 4). Lastly, thieno-pyridine **25** was synthesized from commercially available chloride **12** by palladium-catalyzed carbonylation and side chain construction (Scheme 5).

Analogs were evaluated for inhibitory potency in our PHD2 enzyme assay, which detects proline hydroxylation of a HIF-1α peptide (Table 1).[11] Encouragingly, the initially modeled aza-benzimidazole **14** ($R^1 = R^2 = R^3 = H$) proved to have similar potency to isoquinoline **1** (PHD2 IC_{50} of **1** = 1.40 μM; **14** = 2.82 μM). Since the presumed critical polar elements were already present in this molecule, subsequent analogs were designed to increase potency via addition of lipophilic substituents at R^1, R^2, and R^3.

SAR studies began with a brief scan of substituents at R^1. Replacing the N–H of **14** with N–CH_3 in **15** immediately led to an improvement in potency (IC_{50} = 0.57 μM). Unfortunately, significantly increasing the size of this group further (**16**–**18**) did not lead to additional improvements in activity. Ultimately, phenyl-substituted analog **16** (IC_{50} = 0.29 μM) was chosen as the optimal group for subsequent investigation.

The effects of substitutions at R^2 were investigated next. Improvements in potency via modifications at this position proved difficult. For example, the most active analog prepared in this series, CH_3-substituted compound **19**, was roughly equipotent to **16**

Table 1
PHD2 inhibition by aza-benzimidazole analogs **14**–**22**

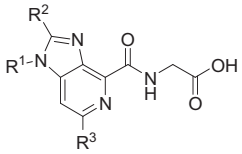

Compound	R^1	R^2	R^3	PHD2[a] (IC_{50}, μM)
14	H	H	H	2.82 ± 0.08
15	CH_3	H	H	0.57 ± 0.05
16	Ph	H	H	0.29 ± 0.19
17	Bn	H	H	0.32 ± 0.13
18	4-BrPh	H	H	0.33 ± 0.11
19	Ph	CH_3	H	0.40 ± 0.04
20	Ph	CF_3	H	5.54 ± 0.95
21	Ph	H	Cl	0.066 ± 0.004
22	Ph	H	Ph	0.003 ± 0.001

[a] IC_{50} values are the average of at least 4 separate experiments.

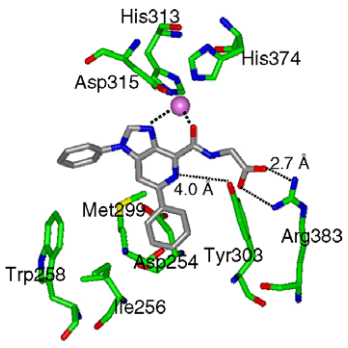

Figure 3. Optimized binding mode of **22** in the active site of PHD2. Fe(II) is shown in pink.

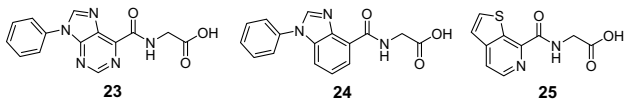

Figure 4. PHD2 inhibition of core-modified analogs **23**–**25**.

(IC_{50} = 0.40 μM). Incorporating a CF_3 group led to significant loss in activity (**20**, IC_{50} = 5.54 μM). This can be rationalized by either steric conflicts of this larger substituent with the protein or a weakened ability to engage Fe(II) or Tyr303 due to electron withdrawal from the imidazole nitrogen(s).

In contrast to R^2, modification of R^3 proved to be beneficial for potency. Chloro-substituted analog **21** (R^1 = Ph, R^2 = H, R^3 = Cl) showed a fourfold increase in potency vs **16** (IC_{50} = 0.066 μM), providing motivation to continue the SAR study. Gratifyingly, it was found that highly potent PHD2 inhibitors could be obtained with aryl substitution. Phenyl-substituted analog **22** proved to be the most active compound prepared in the series (IC_{50} = 0.003 μM).

Molecular modeling studies of diphenyl-substituted analog **22** suggest that in contrast to **14**, only a single preferred binding conformation is accessible. Coordination of Fe(II) is achieved through the imidazole nitrogen, which allows relatively strong van der Waals and hydrophobic contacts with Ile256, Met299, Tyr303, and Asp254 (Fig. 3). The alternative binding mode results in strong steric repulsions between the R^3 phenyl and His313 in this model.

Various alternative core analogs that have weak (or missing) interactions with Fe(II) or Tyr303 were also prepared, and three of these are shown in Figure 4. All analogs lose substantial activity when compared with their aza-benzimidazole counterpart.

Molecular modeling studies. The co-crystal structure of HIF-PHD2 with an isoquinoline inhibitor **1** was used as the starting point for molecular mechanics and dynamics calculations. For docking aza-benzimidazole **14** and analogs, the X-ray structure was used as the template. FLAME[12] was used to generate alignment-based models of **14** starting from the two different conformations corresponding to the minima of the lead. These were obtained by ab initio quantum mechanical calculations, performed for each conformer at B3LYP/6-31G* level, as implemented in Gaussian98 program. Thus, two sets of alignments were obtained, with up to ten different conformations in each set. These were used as the starting points for docking and binding energy assessment using molecular mechanics and dynamics,[13] in conjunction with the AMBER forcefield[14] for the protein and GAFF forcefield[15] for the ligands. Binding affinity calculations were performed using a previously described procedure that treats the protein as flexible. All the protein residues within the first shell (⩽6 Å of any atom) of the docked ligand were allowed to be flexible. These include Asp254, Lys255, Ile256, Trp258, Met299, Ala301, Tyr303, Tyr310, Ile327, Tyr329, Leu343, Val376, Arg383, and Trp389 residues. Crystallographic waters were included in the simulations. A mild restraint was placed on the ligand. Top ranking poses were compared visually and energetically.

In summary, the structure-based design and synthesis of a series of aza-benzimidazoles as PHD2 inhibitors is presented. These efforts resulted in compound **22**, which displayed highly potent inhibition of PHD2 function (IC_{50} = 0.003 μM). In addition, we have gained considerable insight into the structural requirements for efficient PHD2 inhibition.

References and Notes

1. For recent reviews, see: (a) Schofield, C. J.; Ratcliffe, P. J. *Nat. Rev. Mol. Cell. Biol.* **2004**, *5*, 343; (b) Semenza, G. L. *Physiology (Bethesda)* **2004**, *19*, 176; (c) Safran, M., ; Kaelin, W. G., Jr *J. Clin. Invest.* **2003**, *111*, 779; (d) Bruick, R. K. *Genes Dev.* **2003**, *17*, 2614. and references therein.
2. (a) Warshakoon, N. C.; Wu, S.; Boyer, A.; Kawamoto, R.; Renock, S.; Xu, K.; Pokross, M.; Evdokimov, A. G.; Zhou, S.; Winter, C.; Walter, R.; Mekel, M. *Bioorg. Med. Chem. Lett.* **2006**, *16*, 5687; (b) Warshakoon, N. C.; Wu, S.; Boyer, A.; Kawamoto, R.; Sheville, J.; Bhatt, R. T.; Renock, S.; Xu, K.; Pokross, M.; Zhou, S.; Walter, R.; Mekel, M.; Evdokimov, A. G.; East, S. *Bioorg. Med. Chem. Lett.* **2006**, *16*, 5616; (c) Warshakoon, N. C.; Wu, S.; Boyer, A.; Kawamoto, R.; Sheville, J.; Renock, S.; Xu, K.; Pokross, M.; Evdokimov, A. G.; Walter, R.; Mekel, M. *Bioorg. Med. Chem. Lett.* **2006**, *16*, 5598. and references therein.
3. (a) Dann, C. E., III; Bruick, R. K. *Biochem. Biophys. Res. Commun.* **2005**, *338*, 639; (b) Schofield, C. J.; Ratcliffe, P. J. *Biochem. Biophys. Res. Commun.* **2005**, *338*, 617; (c) Berra, E.; Benizri, E.; Ginouves, A.; Volmat, V.; Roux, D.; Pouyssegur, J. *EMBO J.* **2003**, *22*, 4082; (d) Appelhoff, R. J.; Tian, Y. M.; Raval, R. R.; Turley, H.; Harris, A. L.; Pugh, C. W.; Ratcliffe, P. J.; Gleadle, J. M. *J. Biol. Chem.* **2004**, *279*, 38458; (e) Minamishima, Y. A.; Moslehi, J.; Bardeesy, N.; Cullen, D.; Bronson, R. T.; Kaelin, W. G., Jr *Blood* **2007**, *10*, 117812; (f) Percy, M. J.; Furlow, P. W.; Beer, P. A.; Lappin, T. R. J.; McMullin, M. F.; Lee, F. S. *Blood* **2007**, *110*(6), 2193; (g) Percy, M. J.; Zhao, Q.; Flores, A.; Harrison, C.; Lappin, T. R. J.; Maxwell, P. H.; McMullin, M. F.; Lee, F. S. *Proc. Natl. Acad. Sci. U.S.A.* **2006**, *103*(3), 654.
4. McDonough, M. A.; Li, V.; Flashman, E.; Chowdhury, R.; Mohr, C.; Liénard, B. M. R.; Zondlo, J.; Oldham, N. J.; Clifton, I. J.; Lewis, J.; McNeill, L. A.; Kurzeja, R. J. M.; Hewitson, K. S.; Yang, E.; Jordan, S.; Syed, R. S.; Schofield, C. J. *Proc. Nat. Acad. Sci.* **2006**, *103*, 9814.
5. The isoquinoline hydroxyl is desolvated and not satisfied by any proton acceptors.
6. Palmer, B. D.; Smaill, J. B.; Boyd, M.; Boschelli, D. H.; Doherty, A. M.; Hamby, J. M.; Khatana, S. S.; Kramer, J. B.; Kraker, A. J.; Panek, R. L.; Lu, G. H.; Dahring, T. K.; Winters, R. T.; Showalter, H. D. H.; Denny, W. A. *J. Med. Chem.* **1998**, *41*, 5457.
7. Fife, W. K. *J. Org. Chem.* **1983**, *48*, 1375.
8. Penning, T. D.; Chandrakumar, N. S.; Desai, B. N.; Djuric, S. W.; Gasiecki, A. F.; Malecha, J. W.; Miyashiro, J. M.; Russell, M. A.; Askonas, L. J.; Gierse, J. K.; Harding, E. I.; Highkin, M. K.; Kachur, J. F.; Kim, S. H.; Villani-Price, D.; Pyla, E. Y.; Ghoreishi-Haack, N. S.; Smith, W. G. *Bioorg. Med. Chem. Lett.* **2003**, *13*, 1137.
9. Final compounds were in excess of 95% purity as measured by ^{1}H NMR and HPLC. HPLC: (Phenomenex, MAX RP, 4μ, 50 × 2.0 mm, 1 mL/min, A: 0.1% TFA in H_2O, B: 0.1% TFA in MeCN, 10–100% B in 10 min), ^{1}H NMR (Bruker, 400 MHz) in DMSO-d_6 *or* $CDCl_3$.
10. Lam, P. Y. S.; Clark, C. G.; Saubern, S.; Adams, J.; Winters, M. P.; Chan, D. M. T.; Combs, A. *Tetrahedron Lett.* **1998**, *39*, 2941. Regioisomers were separated and identified by NOESY correlations.
11. HIF-PHD2 activity was measured utilizing homogenous time-resolved fluorescence energy transfer technology by detecting the hydroxyl modification of the proline residue of the P564-HIF-1α (Biotin-DLEMLAPYIPMDDDFQL) peptide substrate resulting in recognition by the Europium-tagged Von Hippel-Lindau, Elongin B and Elongin C heterotrimeric complex (VCB-Eu complex). Compound inhibitor potency was determined using 1 nM HIF-PHD2, 100 nM P564-HIF-1α peptide, 0.25 μM 2-OG, 100 μM $FeCl_2$, and 2 mM ascorbic acid in Reaction Buffer (30 mM MES, pH 6, 10 mM NaCl, 10 mM $CaCl_2$, 0.25% Brij-35). The reaction was terminated after 1 h with 50 mM succinic acid in Detection Buffer (50 mM Tris–HCl, pH 8.0, 100 mM NaCl, 0.05% Tween 20, 0.5% NaN_3) containing a final concentration of 25 nM streptavidin-APC and 2.5 nM VCB-Eu. The POC (percentage of control) was determined by comparing the signal from hydroxylated peptide substrate in the enzyme reaction containing inhibitor compound with that from PHD2 enzyme with DMSO vehicle alone, and no enzyme. The data were fit to the 4-parameter model using a Levenburg–Marquardt non-linear regression algorithm.
12. Cho, S.-J.; Sun, Y. *J. Inf. Model* **2006**, *46*, 298. FLAME is implemented as a C++ program, using OpenEye toolkits, OEChem and CASE, available at http://www.eyesopen.com.
13. Lee, M.; Sun, Y. *J. Chem. Theor. Comput.* **2007**, *3*, 1106.
14. Cornell, W. D.; Cieplak, P.; Bayly, C. I.; Gould, I. R.; Merz, K. M.; Ferguson, D. M.; Spellmeyer, D. C.; Fox, T.; Caldwell, J. W.; Kollman, P. A. *J. Am. Chem. Soc.* **1995**, *117*, 5179.
15. Wang, J.; Wolf, R. M.; Caldwell, J. W.; Kollman, P. A.; Case, D. A. *J. Comput. Chem.* **2004**, *25*, 1157.